

The Tactile Contact Lens

R. Kikuuwe, A. Sano, H. Mochiyama, N. Takesue, K. Tsunekawa, S. Suzuki, and H. Fujimoto
Touch Tech Lab Funded By Toyota, Nagoya Institute of Technology, Aichi 466-8555, Japan
kikuuwe@ieee.org

Abstract—This paper introduces a device for enhancing tactile perception of surface undulation. This device, which we call a “tactile contact lens,” is composed of a sheet and numerous pins arranged on one side of the sheet. Our experimental results show that a small bump on a surface can be detected more accurately through this device than by bare finger and than through a flat sheet. A mathematical analysis of this phenomenon suggests two causes of this phenomenon. One cause is a lever-like behavior of the pins, which converts the local inclination of the object surface into the tangential displacement on the skin surface. The second cause is the spatial aliasing effect resulting from the discrete contact, by which the temporal change in the skin surface displacement is efficiently transduced into the temporal change in the skin tissue strain. The result of the analysis is discussed in relation to other sensitivity-enhancing materials, tactile sensing mechanisms, and tactile/haptic display devices.

I. INTRODUCTION

In automobile factories, the surfaces of metal sheets are inspected by craftworkers’ touch. They have long known that they can detect small deflection defects on the surface better when wearing knit work gloves than when using bare hands. A few reports have referred to touch-enhancing phenomena elicited by intermediate objects [1], [2], [3]. It is generally supposed that the main reason for these effects is the reduction of disturbance caused by the friction.

This paper introduces the tactile contact lens (TCL), a device that magnifies the tactile sensation of surface undulation. The basic structure of a tactile contact lens is illustrated in Fig. 1(a). It is composed of a base sheet and numerous pins regularly arranged on one side of the base sheet. When this device is used, the flat side of the base sheet is in contact with a target surface (a surface to be touched), while the other side is pressed by a finger. The device is then moved by the finger across the target surface. The flat side of the base sheet is slippery to facilitate smooth movement on the target surface. The base sheet is flexible enough to follow the undulation on the target surface easily. At the same time, the base sheet is stiff enough to keep the pins perpendicular to the base sheet even under the pressing force applied by the finger. The pins are as tall as permitted by their bending stiffness and resistance to buckling. Fig. 1(b) shows a typical example of the TCL. The pins and the base sheet are made of photo-curing resin (Young’s modulus of approx. 2400 MPa). The size of the base sheet is $25 \times 15 \times 0.3$ mm. Each pin is a cylinder (diameter 1.0 mm, length 3.75 mm) with a semispherical end. The pins are arranged with a pitch of 1.5 mm on the base sheet. A piece of tetrafluoroethylene (TFE) film (thickness 0.09 mm) is glued to the flat side of the base sheet.

We intend to apply this device to the process of sheet metal inspection in the automobile industry. Besides, we expect that the touch-enhancing phenomenon induced by this device will provide useful insight into the mechanistic basis of human tactile sensation and into the design of tactile displays and tactile sensors.

II. EXPERIMENT

Fifteen observers participated in the experiment. All of them were students at Nagoya Institute of Technology. We used the experimental apparatus illustrated in Fig. 2, which is composed of a steel board, a rubber board, a polypropylene (PP) sheet, and a paper disk (a circular piece of paper). On the steel board, a 4-by-3 grid (each 30 mm square) was drawn. Another 4-by-3 grid was drawn on the PP sheet in the same position and of the same size as that on the steel board. The paper disk was placed in either of the 12 cells on the steel board.

The observers were given 6 seconds to detect the cell in which the paper disk existed with the index finger of the right hand. They were asked to respond in a forced choice manner. Trials were performed in either of three conditions: using the TCL shown in Figure 1 (the “lens” condition), using an object identical to the TCL except that it had no pins (the “sheet” condition), and using a bare finger (the “bare-finger” condition). Each observer performed 4 trials under each of three conditions.

The total number of trials under each condition was 60 (4 trials \times 15 observers). Numbers of trials with correct responses in the bare-finger, sheet, and lens conditions were 3, 24, and 49, respectively. The differences were highly significant ($p = 2.50 \times 10^{-6}$ between the bare-finger and sheet conditions; $p = 2.48 \times 10^{-6}$ between the sheet and lens conditions, both by one-tailed Fisher’s exact test).

The increase in the accuracy from the bare-finger condition to the sheet condition is similar to previous findings [1]. The

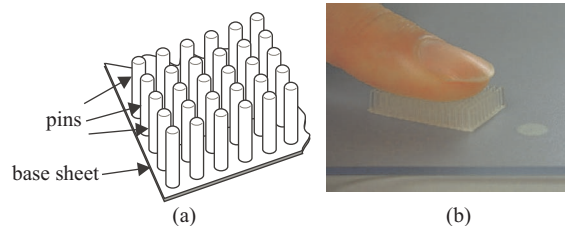


Fig. 1. The tactile contact lens. (a) Basic structure. (b)(c) Photographs of an example prototype.

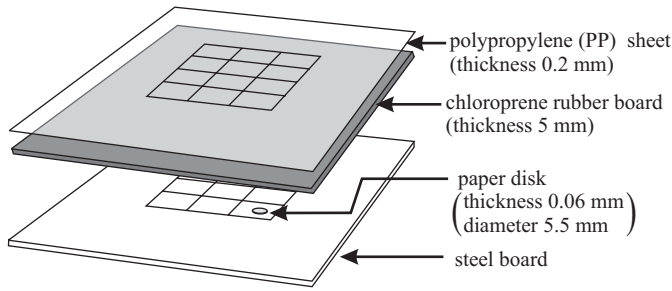


Fig. 2. The experimental apparatus.

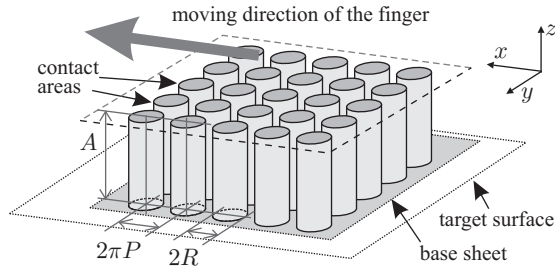


Fig. 3. The coordinate system and the model of the TCL.

reduction of friction may be a cause [2]. On the other hand, the increase in the accuracy from the sheet condition to the lens condition does not seem to have any connection with previous reports. This result suggests that the pins of the TCL have some effects that have not been reported.

III. THEORETICAL EXPLANATION

This section presents an analysis for the sensitivity enhancing effect of the TCL. We aim to show the difference in the strain tensors in the skin that is caused by the presence of the TCL.

We use the following assumptions to build a simplified representation of the finger skin and the TCL: 1) The skin can be approximated as an incompressible, elastic halfspace (the Poisson's ratio, ν , is equal to $1/2$); 2) The base sheet of the TCL always follows the target surface; 3) The pins remain straight, perpendicular to the base sheet; 4) There is no friction between the skin surface and the target surface, nor between the TCL and the target surface; 5) The pins always stick to the skin surface.

A. From target surface geometry to skin surface displacement

We first derive the relation between the target surface geometry and the skin surface displacement. The coordinate system is chosen as shown in Figure 3. Let $h(x, y)$ denote the geometry of the target surface. Let $\mathbf{u}(t, x, y) \in \mathcal{R}^3$ denote the displacement of the skin surface at position (x, y) at time t . Assume that the target surface is moved at velocity $(-V, 0, 0)$ while the skin surface is fixed.

In bare-finger touch, the displacement of the skin surface is determined by

$$\mathbf{u}_B(t, x, y) = h(x + Vt, y) \begin{bmatrix} 0 & 0 & 1 \end{bmatrix}^T \quad (1)$$

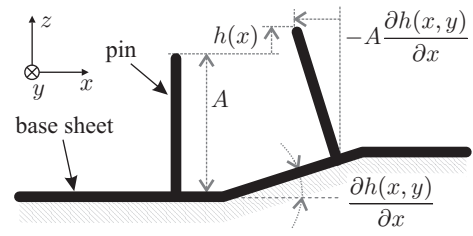


Fig. 4. Displacement of pin-tips caused by surface undulation.

if there is no friction. Here, the subscript B indicates “bare finger.” The Fourier transform of $\mathbf{u}_B(t, x, y)$ is given by

$$\tilde{\mathbf{u}}_B(\omega, \xi, \eta) = \tilde{H}(\omega, \xi, \eta) \begin{bmatrix} 0 & 0 & 1 \end{bmatrix}^T, \quad (2)$$

where

$$\begin{aligned} \tilde{H}(\omega, \xi, \eta) &= \mathcal{F}_{txy} [h(x + Vt, y)](\omega, \xi, \eta) \\ &= \frac{2\pi \tilde{h}}{V} \left(\frac{\omega}{V}, \eta \right) \delta \left(\xi - \frac{\omega}{V} \right). \end{aligned} \quad (3)$$

$\tilde{h}(\xi, \eta)$ is the Fourier transform of $h(x, y)$.

In the case with a TCL, we assume that the displacement of the skin surface can be described as follows:

$$\mathbf{u}_L(t, x, y) = \mathbf{s}(x + Vt, y) m(x, y), \quad (4)$$

where

$$\mathbf{s}(x, y) = \left[-A \frac{\partial h(x, y)}{\partial x}, -A \frac{\partial h(x, y)}{\partial y}, h(x, y) \right]^T, \quad (5)$$

$$m(x, y) = \sum_{\{p, q\} \in \mathcal{Z}^2} r_o(x - 2\pi Pp, y - 2\pi Pq), \quad (6)$$

$$r_o(x, y) = \begin{cases} 1, & \text{if } x^2 + y^2 < R^2 \\ 0, & \text{otherwise} \end{cases}, \quad (7)$$

\mathcal{Z}^2 denotes the set of all pairs of integers, and the subscript L denotes “lens.” Here, a TCL is modeled as illustrated in Figure 3. The pins are cylinders of radius R and length A , and are arranged at a pitch of $2\pi P$. The contact area on the skin surface is the set of points (x, y) for which $m(x, y) = 1$. In the contact area, the normal displacement of the skin surface is determined by the target surface elevation $h(x, y)$. On the other hand, as shown in Figure 4, the tangential displacement is determined by the inclination of the target surface.

The Fourier transform of $\mathbf{u}_L(t, x, y)$ is described as follows:

$$\begin{aligned} \tilde{\mathbf{u}}_L(\omega, \xi, \eta) &= \begin{bmatrix} -jA\xi & -jA\eta & 1 \end{bmatrix}^T \\ &\times \sum_{\{p, q\} \in \mathcal{Z}^2} \tilde{r} \left(\frac{p}{P}, \frac{q}{P} \right) \tilde{H} \left(\omega, \xi - \frac{p}{P}, \eta - \frac{q}{P} \right), \end{aligned} \quad (8)$$

where j is the imaginary unit, $\delta(\cdot)$ is the delta function,

$$\tilde{r}(\xi, \eta) = \frac{\mathcal{F}_{xy} [r_o(x, y)](\xi, \eta)}{4\pi^2 P^2} = \frac{RJ_1(R\sqrt{\xi^2 + \eta^2})}{2\pi P^2 \sqrt{\xi^2 + \eta^2}}, \quad (9)$$

and $J_1(\cdot)$ is the first order Bessel function of the first kind.

B. From skin surface displacement to skin tissue strain

Next, we derive the relation between the skin surface displacement and the skin tissue strain. Let $\mathbf{u}_o(x, y) \in \mathcal{R}^3$ be the surface displacement at position (x, y) , and let $\boldsymbol{\varepsilon}_o(x, y) = [\varepsilon_{xx}, \varepsilon_{yy}, \varepsilon_{zz}, \varepsilon_{xy}, \varepsilon_{yz}, \varepsilon_{zx}]^T \in \mathcal{R}^6$ be the strain at position (x, y) , depth Z . Based on the theory of elasticity [4], the relations among $\mathbf{u}_o(x, y)$, $\mathbf{f}_o(x, y)$, and $\boldsymbol{\varepsilon}_o(x, y)$ are described as follows:

$$\mathbf{u}_o(x, y) = \mathbf{K}_u(x, y) \otimes_{xy} \mathbf{f}_o(x, y), \quad (10)$$

$$\boldsymbol{\varepsilon}_o(x, y) = \mathbf{K}_\varepsilon(x, y) \otimes_{xy} \mathbf{f}_o(x, y), \quad (11)$$

where

$$\mathbf{K}_u(x, y) = \frac{3}{4\pi E(x^2 + y^2)^{3/2}} \begin{bmatrix} 2x^2 + y^2 & xy & 0 \\ xy & x^2 + 2y^2 & 0 \\ 0 & 0 & x^2 + y^2 \end{bmatrix},$$

$$\mathbf{K}_\varepsilon(x, y) = \frac{3}{4\pi E(x^2 + y^2 + Z^2)^{5/2}} \begin{bmatrix} -2x^2 + y^2 + Z^2 & & \\ x^2 - 2y^2 + Z^2 & & \\ x^2 + y^2 - 2Z^2 & & \\ & -6xy & \\ & -6Zy & \\ & -6Zx & \end{bmatrix} \begin{bmatrix} x \\ y \\ Z \end{bmatrix}^T,$$

and \otimes_{xy} denotes the convolution over x and y . Here, E is the Young's modulus and we are assuming the Poisson's ratio is $1/2$. The Fourier transforms of (10) and (11) are respectively written as

$$\tilde{\mathbf{u}}_o(\xi, \eta) = \tilde{\mathbf{K}}_u(\xi, \eta) \tilde{\mathbf{f}}_o(\xi, \eta), \quad (12)$$

$$\tilde{\boldsymbol{\varepsilon}}_o(\xi, \eta) = \tilde{\mathbf{K}}_\varepsilon(\xi, \eta) \tilde{\mathbf{f}}_o(\xi, \eta), \quad (13)$$

where $\tilde{\mathbf{K}}_u(\xi, \eta)$ and $\tilde{\mathbf{K}}_\varepsilon(\xi, \eta)$ are the Fourier transforms of $\mathbf{K}_u(x, y)$ and $\mathbf{K}_\varepsilon(x, y)$, respectively.

Using (12) and (13), we can connect $\mathbf{u}_o(x, y)$ and $\boldsymbol{\varepsilon}_o(x, y)$ by $\tilde{\boldsymbol{\varepsilon}}_o(\xi, \eta) = \tilde{\mathbf{G}}(\xi, \eta) \tilde{\mathbf{u}}_o(\xi, \eta)$ where

$$\tilde{\mathbf{G}}(\xi, \eta) = \tilde{\mathbf{K}}_\varepsilon(\xi, \eta) \tilde{\mathbf{K}}_u(\xi, \eta)^{-1}$$

$$= \frac{e^{-Z\rho}}{\rho} \begin{bmatrix} -j\xi(Z\xi^2 - \rho) & -jZ\xi^2\eta & Z\rho\xi^2 \\ -jZ\xi\eta^2 & -j\eta(Z\eta^2 - \rho) & Z\rho\eta^2 \\ -j\rho\xi(1 - Z\rho) & -j\rho\eta(1 - Z\rho) & -Z\rho^3 \\ -\xi\eta(1 - 2Z\rho) & -\xi^2 - 2\eta^2(1 - Z\rho) & 2jZ\rho^2\eta \\ -\eta^2 - 2\xi^2(1 - Z\rho) & -\xi\eta(1 - 2Z\rho) & 2jZ\rho^2\xi \\ -j\eta(2Z\xi^2 - \rho) & -j\xi(2Z\eta^2 - \rho) & 2Z\rho\xi\eta \end{bmatrix} \quad (14)$$

and $\rho = \sqrt{\xi^2 + \eta^2}$. The function $\tilde{\mathbf{G}}(\xi, \eta)$ is the spatial-frequency response function from the skin surface displacement to the skin tissue strain.

C. From target surface geometry to skin tissue strain

We derive the relation between the target surface geometry and the skin tissue strain. Using (2), we can write $\tilde{\boldsymbol{\varepsilon}}(\omega, \xi, \eta)$ in the case with bare finger as follows:

$$\tilde{\boldsymbol{\varepsilon}}_B(\omega, \xi, \eta) = \tilde{\mathbf{g}}(\xi, \eta) \tilde{H}(\omega, \xi, \eta), \quad (15)$$

where $\tilde{\mathbf{g}}(\xi, \eta)$ is the third column vector of $\tilde{\mathbf{G}}(\xi, \eta)$. On the other hand, $\tilde{\boldsymbol{\varepsilon}}(\omega, \xi, \eta)$ in the case with the TCL is rewritten as

$$\mathcal{F}_{\xi\eta}^{-1}[\tilde{\boldsymbol{\varepsilon}}_L(\omega, \xi, \eta)](x, y) = \mathcal{F}_{\xi\eta}^{-1}[\tilde{\mathbf{k}}(x, y, \xi, \eta) \tilde{H}(\omega, \xi, \eta)](x, y), \quad (16)$$

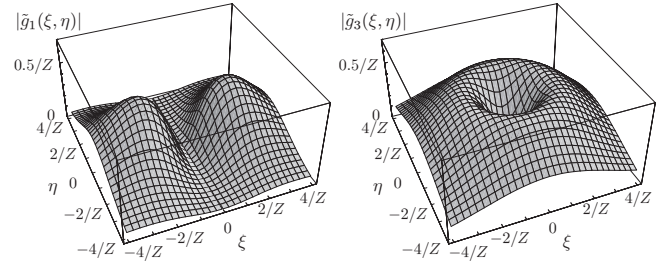


Fig. 5. Plots of functions $|\tilde{g}_1(\xi, \eta)|$ and $|\tilde{g}_3(\xi, \eta)|$, where $\tilde{g}_i(\xi, \eta)$ denotes the i -th element of $\tilde{\mathbf{G}}(\xi, \eta)$.

where

$$\tilde{\mathbf{k}}(x, y, \xi, \eta) = \sum_{\{p, q\} \in \mathcal{Z}^2} e^{j(\frac{p}{P}x + \frac{q}{P}y)} \tilde{r} \left(\frac{p}{P}, \frac{q}{P} \right)$$

$$\times \left(\frac{A}{Z} \tilde{c} \left(\xi + \frac{p}{P}, \eta + \frac{q}{P} \right) + 1 \right) \tilde{\mathbf{g}} \left(\xi + \frac{p}{P}, \eta + \frac{q}{P} \right) \quad (17)$$

$$\tilde{c}(\xi, \eta) = 1 - Z\sqrt{\xi^2 + \eta^2}. \quad (18)$$

Here we used the following identity derived from (14):

$$\tilde{\mathbf{G}}(\xi, \eta) \begin{bmatrix} -j\xi \\ -j\eta \\ 0 \end{bmatrix} = \left(\frac{1}{Z} - \sqrt{\xi^2 + \eta^2} \right) \tilde{\mathbf{G}}(\xi, \eta) \begin{bmatrix} 0 \\ 0 \\ 1 \end{bmatrix} \quad (19)$$

From (15) and (16), we can see that $\tilde{\mathbf{g}}(\xi, \eta)$ and $\tilde{\mathbf{k}}(x, y, \xi, \eta)$ are the frequency response functions from the surface geometry, $\tilde{H}(\omega, \xi, \eta)$, to the strain, $\tilde{\boldsymbol{\varepsilon}}(\omega, \xi, \eta)$, in the case with bare finger and in the case with the TCL, respectively. We can decompose $\tilde{\mathbf{k}}(x, y, \xi, \eta)$ into two terms:

$$\tilde{\mathbf{k}}(x, y, \xi, \eta) = \tilde{a}(\xi, \eta) \tilde{\mathbf{g}}(\xi, \eta) + \tilde{\mathbf{b}}(x, y, \xi, \eta), \quad (20)$$

where

$$\tilde{a}(\xi, \eta) = \tilde{r}(0, 0) \left(\frac{A}{Z} \tilde{c}(\xi, \eta) + 1 \right) \quad (21)$$

$$\tilde{\mathbf{b}}(x, y, \xi, \eta) = \sum_{\{p, q\} \in \mathcal{Z}^2 \setminus \{0, 0\}} e^{j(\frac{p}{P}x + \frac{q}{P}y)} \tilde{r} \left(\frac{p}{P}, \frac{q}{P} \right)$$

$$\times \left(1 + \frac{A}{Z} \tilde{c} \left(\xi + \frac{p}{P}, \eta + \frac{q}{P} \right) \right) \tilde{\mathbf{g}} \left(\xi + \frac{p}{P}, \eta + \frac{q}{P} \right). \quad (22)$$

The reasons for the magnifying effect caused by the TCL can be seen from the comparison between $\tilde{\mathbf{g}}(\xi, \eta)$ and $\tilde{\mathbf{k}}(x, y, \xi, \eta)$.

Equation (20) suggests two causes of the enhancing effect of the TCL. The first term of the right-hand side of (20) represents the magnification of the strain tensor by a scalar factor $\tilde{a}(\xi, \eta)$. This effect is induced by the lever-like behavior of the pins, which converts the local inclination of the target surface into tangential displacement on the skin surface. Equation (19) implies that the normal displacement distribution $\mathbf{u}(x, y) = [0, 0, u_z(x, y)]$ and the tangential displacement distribution $\mathbf{u}(x, y) = [-Z\partial u_z(x, y)/\partial x, -Z\partial u_z(x, y)/\partial y, 0]$ make an equivalent contribution to the strain tensor if $u_z(x, y)$ is band-limited to frequencies sufficiently smaller than $1/Z$. That is, the strain caused by the tangential displacement produced by

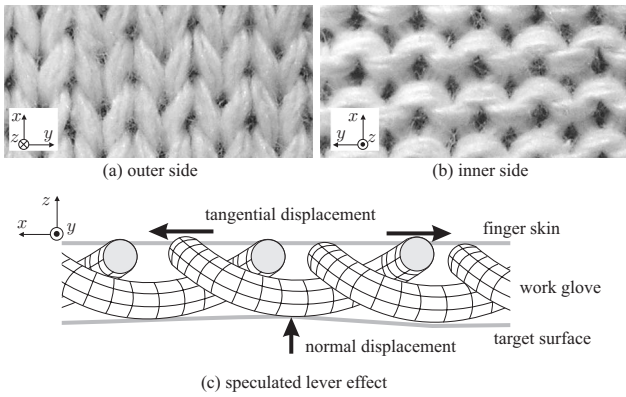


Fig. 6. The structure and mechanics of the work glove fabric (x direction in the figures corresponds to the finger-to-wrist direction).

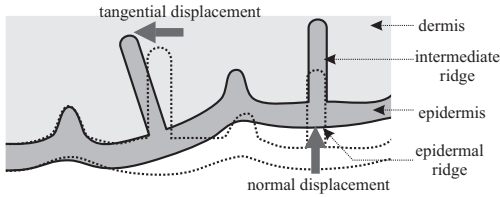


Fig. 7. Speculated lever effect in the human glabrous skin.

the pins is a magnification of the strain caused by the normal displacement produced in bare-finger touch.

The second term of (20), $\tilde{b}(x, y, \xi, \eta)$, represents another cause of the enhancing effect. Carefully looking at (22), we can see that this term can also operate to magnify the tactile stimuli. Fig. 5 shows the gain plots of two of the elements of $\tilde{G}(\xi, \eta)$. As seen in this figure, every element of $\tilde{g}(\xi, \eta)$ has a band-pass filtering characteristic. Therefore, in the low frequency region ($\sqrt{\xi^2 + \eta^2} < 1/Z$, for example), $\tilde{g}(\xi + p/P, \eta + q/P)$ can have a higher gain than $\tilde{g}(\xi, \eta)$ has. As a whole, the gain of $\tilde{b}(x, y, \xi, \eta)$ can be large compared to the gain of $\tilde{g}(\xi, \eta)$. In other words, the spatial aliasing effect, which is caused by the discrete distribution of the contact areas, generates high spatial-frequency components in the skin surface displacement. Because of this, the temporal change in the skin surface displacement is efficiently transduced into the temporal change in the skin tissue strain because incompressible elastic material (in this case, the skin) is a spatial band-pass filter when it is viewed as a transducer from surface displacement to strain.

IV. DISCUSSION

As we mentioned in the beginning of this paper, the sheet metal inspectors in automobile factories know that knit work gloves contribute to the perception of surface undulation. The structure of the fabric of the knit work glove initially suggested the basic structure of the TCL. Fig. 6 show the structure of the work glove fabric. The sheet metal inspectors usually move their hands in the finger-to-wrist direction, which is the x direction in Fig. 6. This structure may have a lever mechanism similar to the TCL as illustrated in Fig. 6(c).

Fearing and Hollerbach [5] predicted that the epidermal ridges play a role in enhancing the amplitude of the strain. This effect is the same as that represented by the second term of (20), i.e., the spatial aliasing effect resulting from the discrete contact. The lever effect also seems to exist in the natural human skin. As shown in Figure 7, the epidermis has ridges projecting into the dermis. It has been speculated [6] that the intermediate ridges act as magnifying levers for the transmission of tactile stimuli. This effect may be similar to the lever effect described by the first term of (20). From a biomimetic perspective, these points will also be worth considering in designing tactile sensors.

Some of the tactile display devices under development use actuated pin arrays for displaying normal displacement (or force) on the skin surface [7], [8], [9]. In contrast, tactile display devices that generate distributed lateral (tangential) displacement (or force) have recently been proposed [10], [11]. Relation (19) implies that the tangential-type tactile displays may be capable of generating a sensation equivalent to that generated by the normal-type tactile displays.

ACKNOWLEDGMENT

This work has been supported by Toyota Motor Corporation. We thank the engineers and craftsmen in Motomachi Plant of Toyota Motor Corporation who motivated and inspired our research.

REFERENCES

- [1] I. E. Gordon and C. Cooper, "Improving one's touch," *Nature*, vol. 256, pp. 203–204, 1975.
- [2] S. J. Lederman, "Improving one's touch"... and more," *Perception and Psychophysics*, vol. 24, no. 2, pp. 154–160, 1978.
- [3] D. A. Perry and H. E. Wright, "Touch enhancing pad," U.S. Patent 4 657 021, 1987.
- [4] A. E. H. Love, *A Treatise on the Mathematical Theory of Elasticity*, 4th ed. Dover, 1927.
- [5] R. S. Fearing and J. M. Hollerbach, "Basic solid mechanics for tactile sensing," *International Journal of Robotics Research*, vol. 4, no. 3, pp. 40–54, 1985.
- [6] N. Cauna, "Nature and functions of the papillary ridges of the digital skin," *Anatomical Record*, vol. 119, pp. 449–468, 1954.
- [7] G. Moy, U. Singh, E. Tan, and R. S. Fearing, "Human psychophysics for teleaction system design," *Haptics-e, The Electronic Journal of Haptics Research* (www.haptics-e.org), vol. 1, no. 3, 2000.
- [8] C. R. Wagner, S. J. Lederman, and R. D. Howe, "A tactile shape display using RC servomotors," in *Proceedings of the 10th Annual meeting of Haptics Interfaces for Teleoperator and Virtual Environment Systems*, 2002, pp. 354–356.
- [9] J. M. Lee, C. R. Wagner, S. J. Lederman, and R. D. Howe, "Spatial low pass filter for pin actuated tactile displays," in *Proceedings of the 11th Symposium on Haptic Interfaces for Virtual Environment and Teleoperator Systems*, 2003, pp. 57–62.
- [10] J. Pasquero and V. Hayward, "STReSS: A practical tactile display system with one millimeter spatial resolution and 700 hz refresh rate," in *Proceedings of The 3rd European Conference on Haptics (EuroHaptics 2003)*, 2003, pp. 94–110.
- [11] J. Pasquero, V. Lévesque, V. Hayward, and M. Legault, "Display of virtual braille dots by lateral skin deformation: A pilot study," in *Proceedings of The 4th European Conference on Haptics (EuroHaptics 2004)*, 2004, pp. 96–103.